

Lateral Stiffness of Reinforced Concrete Interior Flat Plate Connections

Maged A. Youssef *, Mohamed E. Meshaly and Abu Obayed Chowdhury

Western University, Department of Civil and Environmental Engineering,
London, ON N6A 5B9, Canada

Abstract

Flat plates are widely used in Reinforced Concrete structures. To evaluate the lateral stiffness of a flat plate system, the contributing slab width needs to be defined. In this paper, a model that utilizes grillage analysis is proposed to predict the nonlinear lateral behaviour of flat plate structures. The model is utilized to conduct a parametric study to evaluate the effective slab width contributing to the lateral stiffness of residential interior flat plate connections. The studied parameters are span length, bay width, column dimensions, and level of column axial load. Both gravity load designed frames and moment resisting frames are analysed. The effect of the material safety factors is assessed by conducting two sets of analyses using nominal material properties and factored material properties. Equations for estimating the effective slab width contributing to the lateral stiffness of the system are proposed.

Keywords: Slab, Modelling, Stiffness, Flat plate, Effective width, Grillage analysis, Seismic.

* Corresponding author. Tel.: +1 519 661-2111 Ext. 88661; Fax: +1 519 661-3779.

E-mail address: youssef@uwo.ca

1. Introduction

Reinforced concrete (RC) flat slabs simplify the construction process and reduce the overall building height. The National Building Code of Canada [1] allows resisting the lateral loads using moment frames composed of building columns and the flat plates of the different floors. This allowance is limited to low and moderate seismic zones and a maximum building height of 15 m. For other cases, a stiffer lateral force resisting system such as shear walls must be introduced. The flat plate system deforms laterally either as part of a moment resisting frame or as part of a building. Estimation of these deformations requires knowledge of the flat plate system stiffness.

Modelling of flat plates using shell elements to predict their seismic behaviour is cumbersome due to both material and geometric nonlinearities. When subjected to service gravity loads, flat plates behave within the elastic range. They can be modelled using shell elements or beam elements (grillage analysis). O'Brien and Keogh [2] discussed the method of modelling a slab by grids of beam elements to predict its elastic behaviour. Two assumptions related to thin plate theory are made: (1) the depth of the slab remains unchanged, and thus points across the slab thickness deflect vertically by exactly the same amount as points directly above or below them (the assumption is based on the fact that strains in the thickness direction are generally small and have negligible effect on the overall behaviour of the slab) and (2) the deflection of the slab is mainly caused by flexural stresses (effect of shear distortion is ignored). The validity for this method for non-linear analysis was not examined.

A common and practical method for seismic analysis of flat plate systems involves analysing two-dimensional frames. The beam elements of these frames represent an effective slab width, which is critical in defining the stiffness of the slab. The Canadian standard for designing concrete structures [3] specifies an effective slab width factor (α) of 0.2. The Slab effective

width is equal to α times the bay width (B). Based on elastic analysis, Pecknold [4] presented α values for typical interior panels as a function of the column dimension in the span direction (c_1), B, and the span length (L). Based on a limited number of experimental tests, Luo and Durrani [5] proposed Eq. (1) to estimate α corresponding to the total unbalanced moment resulting from lateral loads. They also proposed a reduction factor (χ), Eq. (2), to account for the effect of gravity loads. Their equation did not account for the effects of column axial load and reinforcement ratio. Eq. (1) is unsuitable for estimating the slab lateral stiffness as it corresponds to the total unbalanced moment.

$$\alpha = \frac{1.02 \left(\frac{c_1}{B} \right)}{0.05 + 0.002 \left(\frac{L}{B} \right)^4 - 2 \left(\frac{c_1}{L} \right)^3 - 2.8 \left(\frac{c_1}{L} \right)^2 + 1.1 \left(\frac{c_1}{L} \right)} \quad (1)$$

$$\chi = \left(1 - 0.4 \frac{V_g}{4A_c \sqrt{f'_c}} \right) \quad (2)$$

Where V_g = Direct shear force due to gravity loads, A_c = Area of the critical punching shear section, and f'_c = Compressive strength of concrete.

Hwang and Moehle [6] proposed Eq. (3) to calculate effective slab width (αB) for uncracked slab section based on test results of a flat plate frame. To account for stiffness reduction due to cracking of concrete, αB estimated by Eq. (3) is multiplied by the reduction factor (β), proposed in Eq. (4), that was based on test results of the same flat plate frame.

$$\alpha B = 5c_1 + \frac{L}{4} \quad (3)$$

$$\beta = 5 \frac{c_1}{L} - 0.1 \left(\frac{LL}{40} - 1 \right) \geq \frac{1}{3} \quad (4)$$

Where, LL = service live load, psf

Grossman [7] proposed Eq. (5) to calculate effective slab width (αB) based on test results of a flat plate frame.

$$\alpha B = K_d \left\{ 0.3L + c_1 \left(\frac{B}{L} \right) + \frac{(c_2 - c_1)}{2} \right\} \left(\frac{d}{0.9h} \right) \quad (5)$$

Where, $0.2K_d B \leq \alpha B \leq 0.5K_d B$

K_d = factor considering degradation of stiffness of slabs at various lateral load levels

= 1.1 for 0.125% drift, 1.0 for 0.25% drift, 0.8 for 0.5% drift, and 0.5 for 1% drift

c_2 = column dimension in bay direction

d = effective depth of slab

h = slab thickness

This paper examines the use of grillage analysis to predict the nonlinear seismic behaviour of flat plates. It then provides a comprehensive parametric study for interior residential flat plate connections. It is assumed that these connections are designed according to current design standards, and thus shear failure is excluded. Results from this study are used to propose new effective width formulas suitable for calculating the slab lateral stiffness.

2. Grillage Model

The slab is modelled using a grid of 3D inelastic beam elements. Each beam element represents the concrete and reinforcing bars in a width of the slab equal to the spacing between the elements. Columns are represented using 3D inelastic beam-column elements. The effect of shear deformations on the results is insignificant as compared to flexural deformations [2], and thus is neglected. Spacing between the beam elements depends on the torsional behaviour of the slab [2]. The torsional constant per unit width of any thin plate is twice the second moment of area per unit width. To maintain this ratio, a grid spacing of about 1.25 times the depth of slab should be used. O'Brien and Keogh [2] indicated that this spacing might be impractical and can be increased the up to three times the slab depth without affecting the solution accuracy. The torsional behaviour of slabs without shear reinforcement is expected to be linear up to failure, and thus the torsion rigidity was assumed equal to the elastic value.

Fiber modelling approach was employed to represent the distribution of material nonlinearity along the length and cross-section of each member. The sectional stress-strain state of the elements was obtained through the integration of the nonlinear uniaxial stress-strain response of the individual fibers in which the section was subdivided.

Concrete was modelled using the uniaxial nonlinear constant confinement model of Martinez-Rueda and Elnashai [8]. The constant confining pressure provided by the lateral transverse reinforcement was incorporated through the rules proposed by Mander et al. [9]. The parameters that define the model are: concrete compressive strength (f'_c), concrete tensile strength (f_t), strain at peak stress (ε_o), and confinement factor (k_c). A uniaxial bilinear stress-strain model was used to model the reinforcing bars. The parameters defining the model are: the modulus of elasticity (E_s), yield strength (f_y), and strain hardening parameter (μ).

Shear failure is excluded as it is assumed that slabs are designed according to current design standards. Flexural failure occurs when the unconfined concrete of the slab reaches its crushing strain that ranges between 0.003 and 0.004 [10].

The proposed technique for modelling a flat plate using grillage analysis is validated using the results of two experiments by Robertson and Durrani [11]. The experiments represent an isolated interior (8I) and an edge (9E) flat plate slab-column connection with slab dimension of 2895.6 x 1981.2 and 1447.8 x 1981.2 mm, respectively. SeismoStruct computer program [12] is utilized to conduct the non-linear analysis. The test setup is shown in Fig. 1. The 254 mm square column is hinged at its base. Roller supports are provided at the edges of the slabs. Slab thickness, column height, column reinforcement, and column ties were 114.3 mm and 1420 mm, 8-22 mm bars, and 10 mm bars spaced at 76 mm, respectively. Properties of concrete and reinforcing bars are given in Table 1. Grid spacing was chosen as 241.3 mm and 247.65 mm along the longitudinal and transverse directions, respectively. The grid models of slabs of specimens (8I) and (9E) are shown in Fig. 2. The notations given for each beam element corresponds to its properties as summarized in Table 2. Point loads were applied at each node of the grid to model the gravity load of the slab. Column self-weight was applied at the end node of the column element. Static pushover analyses were then performed by incrementally increasing the lateral deformation at the location of the lateral load P.

Comparisons between the analytical lateral load-drift curves and the experimental one are shown in Fig. (3). It is clear that the analytical model was able to accurately predict behaviour of the tested slabs up to failure.

3. Nominal and Factored Lateral Stiffness of a Flat Plate System

The validated grillage analysis is used to conduct a parametric study to evaluate the effective width that can be used to estimate the nominal and factored stiffness of a flat plate system. Two types of connections are considered; connections designed for gravity loads and those designed for lateral loads. Connections similar to the one shown in Fig. 1 are designed and investigated. The considered geometric parameters, which have significant effect on the effective slab width, are: span length, bay width, and column dimension in the span direction. Values for the considered parameters are shown in Table 3. The story height is taken as 3 m. While varying one geometric parameter, the other two parameters are assumed to remain constant at the mean value. The variation of the column axial load from floor to floor was considered by designing connections with different column axial loads. Nominal and factored ratios of column axial loads relative to that of the column supporting one storey $\left(\frac{P}{P_1} \text{ and } \frac{P_f}{P_{f1}} \right)$ are shown in Table 3.

Compressive strength of concrete and yield strength of steel are taken as 25 and 400 MPa, respectively. These values are widely used for flat plate structures.

3.1 Gravity load design of flat plates

The service dead load of the slab is assumed to be composed of the self-weight of the slab and a uniform partition weight of 1 kPa. The service live loads are taken as 1.9 kPa and 1.0 kPa for the floor and roof to represent residential buildings. The slab of each connection is designed for the gravity load composed of the dead and live loads using the direct design method of

Canadian standard for designing concrete structures [3]. The layouts of the top and bottom slab reinforcements are shown in Fig. 4 and their amounts are given in Table 4.

3.2 Lateral load design of flat plates

The slab-column connection of each configuration is modelled as an elastic 2D, Fig. 1, using the sectional properties recommended in Canadian standard for designing concrete structures [3]. The effective moment of inertia for the slabs, I_e was taken as 0.2 times the gross moment of inertia, I_g . For the column, I_e was taken equal to $\alpha_c I_g$ where α_c is a factor to account for the effect of the column axial load, P_s and is given by Eq. (6).

$$\alpha_c = 0.5 + 0.6 \frac{P_s}{f'_c A_g} \leq 1.0 \quad (6)$$

Where, A_g = gross area of column section

The lateral load-inter-storey drift curve of a typical concrete building designed according to current seismic standards is shown in Fig. 5. The behaviour is expected to be elastic until a yield load of V_y . This is followed by plastic deformations until reaching failure. The maximum inter-storey drift can be assumed to be 2.5% [1]. Based on the equal displacement principle, V_y can be calculated based on the corresponding elastic load $V_e \left(V_y = \frac{V_e I_E}{R_d R_0} \right)$. The importance factor I_E , ductility factor R_d and over-strength factor R_0 are taken as 1, 1.5 and 1.3 [1]. Service lateral loads corresponding to a drift of 2.5% in both directions are determined and used to design the slab. The reinforcement values are given in Table 5.

3.3 Columns

Square columns of dimensions 600, 700, and 800 mm reinforced with 16-25M, 16-30M, and 16-25M bars, respectively, are assumed for all connections. 10M ties are used for all columns. Their spacing is 375 mm for the 600 mm and 800 mm columns and 475 mm for the 700 mm column. The strong column-weak slab requirement is satisfied for all connections.

3.4 Analytical modelling and results

SeismoStruct computer program [12] is used to model each connection using the proposed grillage method. A grid spacing of 250 mm was used for both 4×6 m and 6×6 m slabs. For 8×6 m slab, the grid spacing was increased to 333.33 mm. Gravity loads are first applied and then static pushover analysis was performed until failure. Failure was defined by reaching a concrete strain of 0.0035 [3]. The lateral stiffness of the connections shown in Table 3 is investigated in this section. Effect of drift level on effective slab width is also investigated.

3.4.1 Analytical results

Typical lateral load-drift curves corresponding to nominal and factored material properties and different axial load ratios are shown in Figs. 6a and 6b. Figure 6a shows that varying $\frac{P}{P_1}$ from 14 to 1 increases the ultimate lateral load corresponding to nominal material properties from 25 kN to 50 kN for GL flat plates and 50 kN to 100 kN for MRF flat plates. The corresponding increase considering factored material properties (Fig. 6b) is from 12.50 kN to 43.75 kN for GL

flat plates and from 37.5 kN to 75 kN for MRF flat plates. These curves maintain constant slope until yield points that correspond to a drift of about 0.5%. A flat plateau follows this until a drift of 2.5% is reached. MRF flat plates have higher reinforcement ratios as compared to GL flat plates. This resulted in an increase in their lateral stiffness as compared to GL flat plates. The nominal and factored effective slab width factor (α_n and α_r) that correspond to drift levels of 0.5%, 1.5% and 2.5% are calculated for all considered connections. This is achieved by applying the load corresponding to drift levels of 0.5%, 1.5%, and 2.5% to a 2D elastic frame model and varying the slab width until matching drifts are achieved. Nominal and factored effective slab width factors are shown in Table 6. For the considered cases, α_n and α_r were found to vary from 0.012 to 0.282 and from 0.008 to 0.223, respectively.

3.4.2 Discussion of analytical results

Variations of nominal effective slab width factors with span length, bay width and column dimension at different axial load ratios and drift levels for GL and MRF flat plates are shown in Figs. 7a-7c at 0.5% drift. These curves show that the nominal effective slab width factors decrease as the axial load of column increases for GL and MRF flat plates. The factors for MRF flat plates are greater than those for GL flat plates. This can be referred to the delay in yielding and the increase of the lateral stiffness of the MRF flat plate because of its higher reinforcement ratio.

Fig. 7a shows that α_n vary from 0.052 to 0.193 for GL flat plates and 0.095 to 0.266 for MRF flat plates as the span length changes from 4 m to 8 m. This is likely due to increase in the top reinforcement ratio with the increase of the span length

Fig. 7b shows that α_n vary from 0.190 to 0.065 for GL flat plates and 0.282 to 0.101 for MRF flat plates as the bay width changes from 4 m to 8 m. Increasing the bay width increases gravity moments and eventually the top reinforcement ratio.

Fig. 7c shows that α_n vary from 0.118 to 0.063 for GL flat plates and 0.156 to 0.098 for MRF flat plates as the column dimension changes from 600 mm to 800 mm. Column dimensions are found to have minor effects on α_n for GL and MRF flat plates at a particular axial load ratio.

Variations of nominal effective slab width factors with span length, bay width and column dimension at different drift levels for GL and MRF flat plates are shown in Figs. 8a-8c at $\frac{P}{P_1} = 1$.

These curves show that the effective width factors decrease as the level of drift increase for MRF and GL flat plates due to the gradual reduction of lateral stiffness of flat plate system.

Fig. 8a shows that α_n vary from 0.028 to 0.193 for GL flat plates and 0.044 to 0.266 for MRF flat plates as the span length changes from 4 m to 8 m. Fig. 8b shows that α_n vary from 0.190 to 0.032 for GL flat plates and 0.282 to 0.044 for MRF flat plates as the bay width changes from 4 m to 8 m.

Fig. 8c shows that α_n vary from 0.032 to 0.118 for GL flat plates and 0.044 to 0.156 for MRF flat plates as the column dimension changes from 600 mm to 800 mm. Column dimensions are found to have minor effects on α_n for GL and MRF flat plates at a particular axial load ratio.

3.5 Effective slab width

Using the calculated effective slab width factor suitable for lateral stiffness, two expressions are developed to estimate α_n and α_r for different configurations. It is found that the effective

width factor is proportional to parabolic functions of the axial load of column $\left(\frac{P}{P_1}\right)$, drift level (D), span length (L), and bay width (B), respectively. This led to assuming that effective slab width factor (α) is equal to the following expression.

$$\alpha = R_a R_d (A_7 L^2 + A_8 L + A_9) (A_{10} B^2 + A_{11} B + A_{12}) \quad (7)$$

Where,

$$R_a = A_1 \left(\frac{P}{P_1}\right)^2 + A_2 \left(\frac{P}{P_1}\right) + A_3$$

$$R_d = A_4 D^2 + A_5 D + A_6$$

The values of A_1 through A_{12} were determined using regression analysis such that the difference between the analytical values for α and the values determined from Eq. (7) is minimized. The expressions to estimate α_n for GL and MRF are given by Eqs. (8) and (9), respectively. α_r can be estimated by multiplying α_n by 0.73 and 0.79 for GL and MRF flat plates, respectively.

$$\alpha_n = 10^{-16} R_a R_d (308L^2 - 2338L + 8415) (560B^2 - 7716B + 31235) \quad (8)$$

Where,

$$R_a = 3 \left(\frac{P}{P_1}\right)^2 - 209 \left(\frac{P}{P_1}\right) + 4764$$

$$R_d = 1761D^2 - 8676D + 13043$$

D = Drift (%)

L = span length (m)

B = bay width (m)

$$\alpha_n = 10^{-16} R_a R_d (609L^2 - 5517L + 19687)(627B^2 - 8764B + 35025) \quad (9)$$

Where,

$$R_a = 3\left(\frac{P}{P_1}\right)^2 - 171\left(\frac{P}{P_1}\right) + 4736$$

$$R_d = 1505D^2 - 7429D + 11265$$

The predicted values by Eqs. (8) and (9) are compared with analytical results in Tables 7 and 8, respectively. The comparisons are also shown in Fig. 9. It shows minor deviation of analytical results from the predicted values of equations (8) and (9) (deviation of ± 0.038).

The predictions of Eq. (8) are compared with analytical models that were based on experimental results [6, 11, 13, 14, 15, 16]. The comparison is shown in Table 9. Maximum deviation of Eq. (3) from Eq. (8) is -0.105 for specimen b3 by Hwang and Moehle [6]. On the other hand, maximum deviation of Eq. (5) from Eq. (8) is 0.105 for specimen 3 by Pan and Moehle [13].

4. Conclusion

In this paper, the use of grillage analysis to predict the nonlinear seismic behaviour of flat plates is explained and validated using available experimental results. A parametric study is then conducted to evaluate the effective slab width required to calculate the lateral stiffness corresponding to nominal and factored material properties for different spans, bay widths, column dimensions, column axial loads, and drift levels. Two sets of flat plate frames are designed. They represent flat plate structures designed for gravity loads and horizontal loads. Each structure is modelled using grillage analysis and is subjected to an increasing lateral load.

The nominal and factored effective slab width factors are found to increase with the increase of flat plate span and decrease with the increase of bay width. Column dimensions are found to have minor effects on their values. They are also found to decrease as the axial loads of column and levels of drift increase. GL flat plates had smaller values as compared to MRF flat plates. Expressions for nominal and factored effective slab width factors are proposed. Their predictions are validated using available experimental results and found to be adequate. Nominal and factored effective slab width factors calculated in this study are applicable to the range of parameters considered and care should be taken when using them for other cases.

References

- [1] NBCC (2010), *National Building Code of Canada*, Institute for Research in Construction, National Research Council of Canada, Ottawa.
- [2] O'Brien E. J. and Keogh D. L. (1999), *Bridge Deck Analysis*, E & FN Spon, London, UK.
- [3] A23.3-04 (2004), *Design of Concrete Structures*, Canadian Standards Association, Mississauga.
- [4] Pecknold D. A. (1975), "Slab effective width for equivalent frame analysis", *ACI Journal*, **72**(4), 135-137.
- [5] Luo Y. H. and Durrani A. J. (1995), "Equivalent beam model for flat-slab buildings-part I: interior connections", *ACI Structural Journal*, **92**(1), 115-124.

- [6] Hwang S. J. and Moehle J. P. (1993), “An experimental study of flat-plate structures under vertical and lateral loads”, *Earthquake Engineering Research Center*, University of California at Berkeley, Berkeley, California, USA, Report No. UCB/EERC-93/03, pp. 27-28, 36 and 59.
- [7] Grossman J. S. (1997), “Verification of proposed design methodologies for effective width of slabs in slab-column frames”, *ACI Structural Journal*, **94**(2), 181-196.
- [8] Martinez-Rueda J. E. and Elnashai A. S. (1997), “Confined concrete model under cyclic load”, *Materials and Structures*, **30**(197), 139-147.
- [9] Mander J. B., Priestley M. J. N. and Park R. (1988), “Theoretical stress-strain model for confined concrete”, *ASCE Journal of Structural Engineering*, **114**(8), 1804-1826.
- [10] Park R. and Paulay T. (1972), *Reinforced Concrete Structures*, JOHN WILEY & SONS, INC., Canada.
- [11] Robertson I. N. and Durrani A. J. (1990), “Seismic response of connections in indeterminate flat-slab subassemblies”, Ph.D. Dissertation, Rice University, Houston, Texas.
- [12] SeismoSoft (2007) “Seismostruct- A computer program for static and dynamic nonlinear analysis of framed structures”, Available from URL: <http://www.seissoft.com/SeismoStruct/index.htm>.
- [13] Pan A. D. and Moehle J. P. (1988), “Reinforced concrete flat plates under lateral loading: an experimental study including biaxial effects”, *Earthquake Engineering Research Center*, University of California at Berkeley, Berkeley, California, USA, Report No. UCB/EERC-88/16, 262 pp.

[14] Farhey D. N., Adin M. A. and Yankelevsky D. Z. (1993), "RC flat slab-column subassemblages under lateral loading", *ASCE Journal of Structural Engineering*, **119**(6), 1903-1916.

[15] Morrison D. G. and Sozen M. A. (1981), "Response of reinforced concrete plate-column connections to dynamic and static horizontal loads", *Civil Engineering Studies, Structural Research Series*, University of Illinois, Urbana-Champaign, Illinois, USA, Report No. 490.

[16] Islam S. and Park R. (1976), "Tests on slab-column connections with shear and unbalanced flexure", *ASCE Journal of Structural Division*, **102**(3), 549-568.

Table 1: Properties of concrete and reinforcement (Robertson and Durrani, 1990).

Materials	Properties	Slab	Column
Concrete	Compressive strength (MPa)	39.3	39.3
	Tensile strength (MPa)	2.068	2.068
	Strain at peak stress (mm/mm)	0.002	0.002
	Confinement factor	1.00	1.23
Reinforcement	Modulus of elasticity (MPa)	203127	
	Yield strength (MPa)	525	
	Strain hardening parameter	0.001	

Table 2: Properties of beam elements modelling Robertson and Durrani (1990) tests.

Designation	Width (mm)	Reinforcement area (mm ²)	
		Top	Bottom
S1	123.825	22.44	23.56
S2	247.650	44.88	47.12
S3	247.650	64.52	47.12
S4	247.650	117.83	68.88
S5	120.650	20.14	20.16
S6	241.300	40.29	40.33
S7	241.300	65.61	40.33
S8	241.300	86.10	63.85

Table 3: Properties of considered connections

Connection	Span (m)	Bay width (m)	Square Column dimension (mm)	Slab thickness (mm)	Nominal axial load ratio, $\frac{P}{P_1}$			Factored axial load ratio, $\frac{P_f}{P_{f1}}$		
C1	4	6	700	200						
C2	6	6	700	200						
C3	8	6	700	270						
C4	6	4	700	200	1	7	14	1	7	14
C5	6	8	700	270						
C6	6	6	600	200						
C7	6	6	800	200						

Table 4: Top and bottom reinforcements of connections designed for gravity load only.

Connection	L (m)	B (m)	L ₁ (m)	B ₁ (m)	A _{s1}	A _{s2}	A _{s3}	A _{s4}	A _{s5}
C1	4	6	3	2	3-10M@200 mm	10M@200 mm	10M@250 mm	10M@250 mm	10M@250 mm
C2	6	6	4	3	3-15M@250 mm	15M@250 mm	15M@500 mm	10M@200 mm	10M@250 mm
C3	8	6	6	3	3-15M@170 mm	15M@170 mm	15M@370 mm	15M@300 mm	15M@370 mm
C4	6	4	4	2	3-10M@135 mm	10M@135 mm	10M@250 mm	10M@250 mm	10M@250 mm
C5	6	8	4	3	3-15M@225 mm	15M@225 mm	15M@370 mm	15M@370 mm	15M@370 mm
C6	6	6	4	3	3-15M@245 mm	15M@245 mm	15M@500 mm	10M@195 mm	10M@250 mm
C7	6	6	4	3	3-15M@250 mm	15M@250 mm	15M@500 mm	10M@205 mm	10M@250 mm

Table 5: Top and bottom reinforcements of connections designed for gravity and lateral loads.

Connection	L (m)	B (m)	L ₁ (m)	B ₁ (m)	A _{s1}	A _{s2}	A _{s3}	A _{s4}	A _{s5}
C1	4	6	3	2	5-20M@135 mm	20M@135 mm	15M@500 mm	15M@155 mm	15M@500 mm
C2	6	6	4	3	7-20M@125 mm	20M@125 mm	15M@500 mm	15M@200 mm	10M@250 mm
C3	8	6	6	3	9-20M@105 mm	20M@105 mm	15M@370 mm	15M@215 mm	15M@370 mm
C4	6	4	4	2	5-20M@140 mm	20M@140 mm	15M@500 mm	15M@210 mm	15M@500 mm
C5	6	8	4	3	9-20M@105 mm	20M@105 mm	15M@370 mm	15M@155 mm	15M@370 mm
C6	6	6	4	3	7-20M@130 mm	20M@130 mm	15M@500 mm	15M@205 mm	10M@250 mm
C7	6	6	4	3	7-20M@120 mm	20M@120 mm	15M@500 mm	15M@195 mm	10M@250 mm

Table 6: Nominal and factored effective slab width factors (α_n and α_r) for different connections.

Connection	$\frac{P}{P_1}$	$\frac{P_f}{P_{f1}}$	Flat plate system	α_n			α_r		
				Drift (%)			Drift (%)		
				0.5	1.5	2.5	0.5	1.5	2.5
C1	1	1	GL	0.078	0.039	0.028	0.057	0.028	0.020
			MRF	0.120	0.061	0.045	0.095	0.048	0.035
	7	7	GL	0.065	0.028	0.019	0.047	0.020	0.013
			MRF	0.108	0.048	0.033	0.085	0.038	0.026
	14	14	GL	0.052	0.021	0.012	0.037	0.153	0.008
			MRF	0.095	0.039	0.023	0.075	0.031	0.018
C2	1	1	GL	0.117	0.055	0.032	0.085	0.040	0.023
			MRF	0.155	0.074	0.044	0.122	0.058	0.035
	7	7	GL	0.090	0.039	0.023	0.065	0.028	0.016
			MRF	0.128	0.056	0.034	0.101	0.044	0.027
	14	14	GL	0.065	0.025	0.015	0.047	0.018	0.010
			MRF	0.101	0.040	0.024	0.080	0.032	0.019
C3	1	1	GL	0.193	0.082	0.048	0.140	0.059	0.035
			MRF	0.266	0.114	0.067	0.210	0.090	0.053
	7	7	GL	0.167	0.067	0.039	0.121	0.048	0.028
			MRF	0.236	0.095	0.056	0.186	0.075	0.044
	14	14	GL	0.143	0.055	0.032	0.104	0.040	0.023
			MRF	0.210	0.082	0.049	0.166	0.065	0.039
C4	1	1	GL	0.190	0.092	0.055	0.138	0.067	0.040
			MRF	0.282	0.137	0.082	0.223	0.108	0.065
	7	7	GL	0.160	0.071	0.042	0.116	0.051	0.030
			MRF	0.250	0.111	0.066	0.197	0.088	0.052
	14	14	GL	0.132	0.054	0.032	0.096	0.039	0.023
			MRF	0.220	0.091	0.054	0.174	0.072	0.043
C5	1	1	GL	0.105	0.049	0.036	0.076	0.035	0.026
			MRF	0.145	0.069	0.051	0.114	0.054	0.040
	7	7	GL	0.090	0.039	0.026	0.065	0.028	0.018
			MRF	0.127	0.056	0.038	0.100	0.044	0.030
	14	14	GL	0.076	0.030	0.018	0.055	0.021	0.013
			MRF	0.112	0.045	0.027	0.088	0.035	0.021
C6	1	1	GL	0.118	0.056	0.032	0.086	0.040	0.023
			MRF	0.156	0.075	0.044	0.123	0.059	0.035
	7	7	GL	0.091	0.039	0.022	0.066	0.028	0.016
			MRF	0.128	0.056	0.033	0.101	0.044	0.026
	14	14	GL	0.066	0.026	0.015	0.048	0.018	0.010
			MRF	0.101	0.040	0.024	0.080	0.032	0.019
C7	1	1	GL	0.116	0.056	0.033	0.084	0.040	0.024
			MRF	0.153	0.074	0.044	0.121	0.058	0.035
	7	7	GL	0.090	0.038	0.023	0.065	0.027	0.016
			MRF	0.126	0.054	0.033	0.099	0.043	0.026
	14	14	GL	0.063	0.025	0.014	0.045	0.018	0.010
			MRF	0.098	0.039	0.023	0.077	0.031	0.018

Table 7: Comparison of the predicted values of equation (8) and the analytical results.

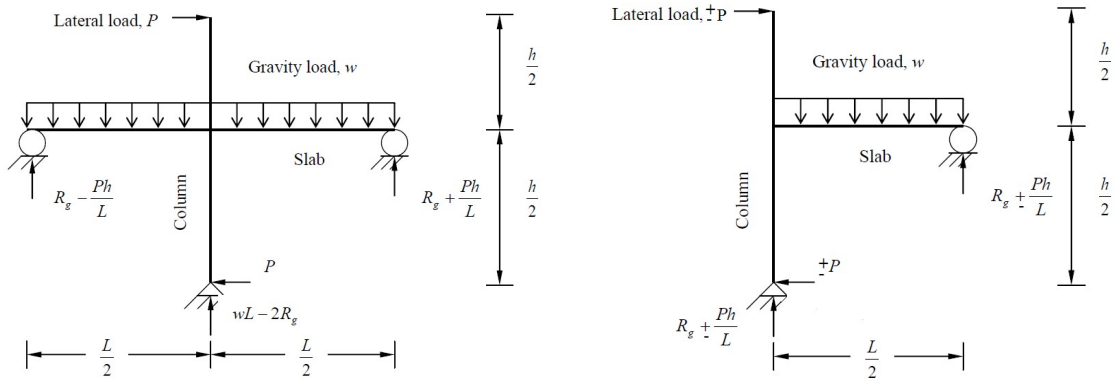
Connection	$\frac{P}{P_1}$	α_n			Eq.			Deviation		
		Drift (%)			Drift (%)			Drift (%)		
		0.5	1.5	2.5	0.5	1.5	2.5	0.5	1.5	2.5
C1	1	0.078	0.039	0.028	0.085	0.037	0.022	-0.007	0.002	0.006
	7	0.065	0.028	0.019	0.065	0.028	0.017	0.000	0.000	0.002
	14	0.052	0.021	0.012	0.052	0.021	0.012	0.000	0.000	0.000
C2	1	0.117	0.055	0.032	0.117	0.051	0.030	0.000	0.004	0.002
	7	0.090	0.039	0.023	0.089	0.039	0.023	0.001	0.000	0.000
	14	0.065	0.025	0.015	0.065	0.028	0.016	0.000	-0.003	-0.001
C3	1	0.193	0.082	0.048	0.201	0.087	0.051	-0.008	-0.005	-0.003
	7	0.167	0.067	0.039	0.153	0.067	0.039	0.014	0.000	0.000
	14	0.143	0.055	0.032	0.112	0.049	0.029	0.031	0.006	0.003
C4	1	0.190	0.092	0.055	0.213	0.093	0.055	-0.023	-0.001	0.000
	7	0.160	0.071	0.042	0.162	0.071	0.042	-0.002	0.000	0.000
	14	0.132	0.054	0.032	0.119	0.052	0.030	0.013	0.002	0.002
C5	1	0.105	0.049	0.036	0.122	0.053	0.032	-0.017	-0.004	0.004
	7	0.090	0.039	0.026	0.093	0.040	0.024	-0.003	-0.001	0.002
	14	0.076	0.030	0.018	0.069	0.030	0.018	0.007	0.000	0.000
C6	1	0.118	0.056	0.032	0.117	0.051	0.030	0.001	0.005	0.002
	7	0.091	0.039	0.022	0.089	0.039	0.023	0.002	0.000	-0.001
	14	0.066	0.026	0.015	0.065	0.028	0.016	0.001	-0.002	-0.001
C7	1	0.116	0.056	0.033	0.116	0.051	0.030	0.000	0.005	0.003
	7	0.090	0.038	0.023	0.089	0.038	0.023	0.001	0.000	0.000
	14	0.063	0.025	0.014	0.065	0.028	0.016	-0.002	-0.003	-0.002

Table 8: Comparison of the predicted values of equation (19) and the analytical results.

Connection	$\frac{P}{P_1}$	α_n			Eq.			Deviation		
		Drift (%)			Drift (%)			Drift (%)		
		0.5	1.5	2.5	0.5	1.5	2.5	0.5	1.5	2.5
C1	1	0.120	0.061	0.045	0.134	0.059	0.034	-0.014	0.002	0.011
	7	0.108	0.048	0.033	0.108	0.048	0.028	0.000	0.000	0.005
	14	0.095	0.039	0.023	0.095	0.039	0.023	0.000	0.000	0.000
C2	1	0.155	0.074	0.044	0.155	0.069	0.041	0.000	0.005	0.003
	7	0.128	0.056	0.034	0.126	0.056	0.033	0.002	0.000	0.001
	14	0.101	0.040	0.024	0.101	0.044	0.026	0.000	-0.004	-0.002
C3	1	0.266	0.114	0.067	0.266	0.117	0.070	0.000	-0.003	-0.003
	7	0.236	0.095	0.056	0.215	0.095	0.056	0.021	0.000	0.000
	14	0.210	0.082	0.049	0.172	0.076	0.045	0.038	0.006	0.004
C4	1	0.282	0.137	0.082	0.309	0.137	0.082	-0.027	0.000	0.000
	7	0.250	0.111	0.066	0.250	0.111	0.066	0.000	0.000	0.000
	14	0.220	0.091	0.044	0.201	0.089	0.053	0.019	0.002	-0.009
C5	1	0.145	0.069	0.051	0.157	0.069	0.041	-0.012	0.000	0.010
	7	0.127	0.056	0.038	0.127	0.056	0.033	0.000	0.000	0.005
	14	0.112	0.045	0.027	0.102	0.045	0.027	0.010	0.000	0.000
C6	1	0.156	0.075	0.044	0.156	0.069	0.041	0.000	0.006	0.003
	7	0.128	0.056	0.033	0.126	0.056	0.033	0.002	0.000	0.000
	14	0.101	0.040	0.024	0.101	0.044	0.026	0.000	-0.004	-0.002
C7	1	0.153	0.074	0.044	0.155	0.069	0.041	-0.002	0.005	0.003
	7	0.126	0.054	0.033	0.126	0.055	0.033	0.000	-0.001	0.000
	14	0.098	0.039	0.023	0.101	0.044	0.026	-0.003	-0.005	-0.003

Table 9: Comparison of the predicted values of equation (8) with different models.

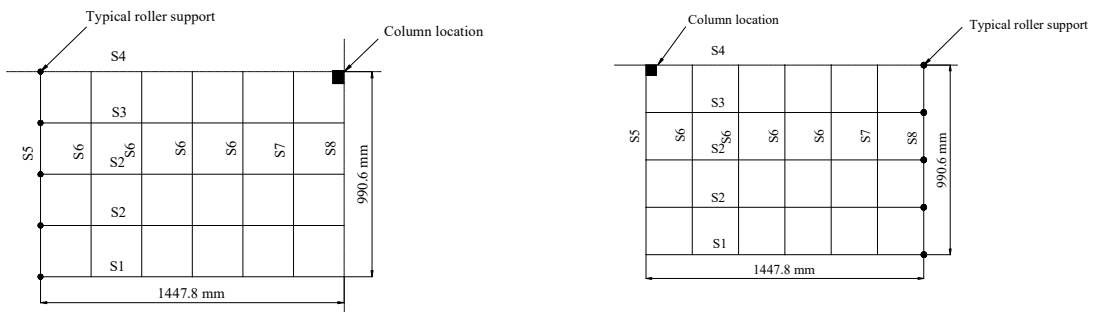
Experiments	Specimens	L (m)	B (m)	c_1 (mm)	$\frac{P}{P_1}$	Drift (%)	α_n		
							Eq.		
							(3)	(5)	(8)
Pan and Moehe (1988)	3	3.65	3.65	274	1	0.5	0.208	0.280	0.175
Robertson and Durrani (1990)	8I	2.89 1.98	1.98 2.89	254			0.335 0.203	0.374 0.238	0.320 0.283
Farhey et al. (1993)	1	2.68	2.68	300			0.269	0.273	0.265
Morrison and Sozen (1981)	S1	1.82	1.82	305			0.362	0.332	0.411
Hwang and Moehe (1993)	b3	2.74 1.82	1.82 2.74	244			0.348 0.203	0.400 0.266	0.343 0.308
Islam and Park (1976)	1	2.74 2.28	2.28 2.74	229			0.267 0.208	0.310 0.244	0.298 0.279



a. Interior connection (8I)

b. Exterior connection (9E)

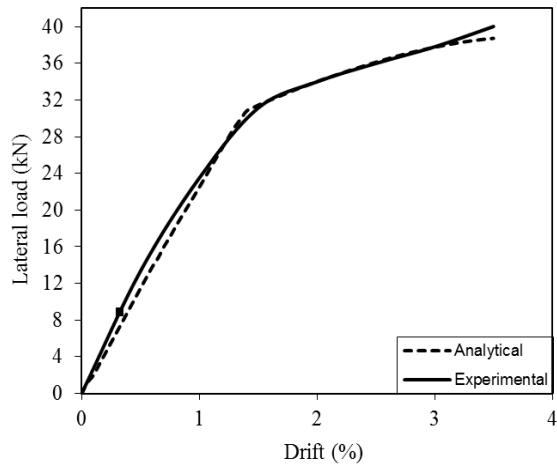
Fig. 1 Slab-column connection subjected to gravity and lateral loads



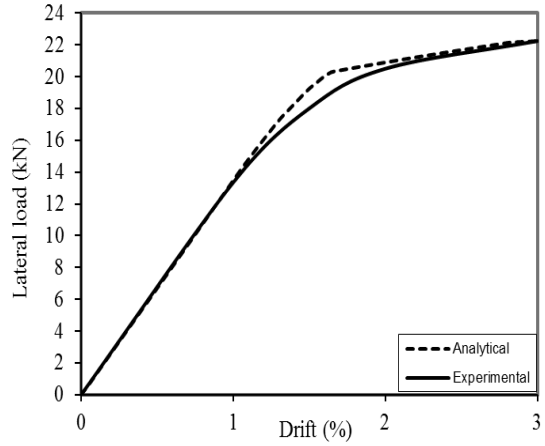
a. Quarter of specimen 8I

b. half of specimen 9E

Fig. 2 Grid model of a tested by Robertson and Durrani (1990)

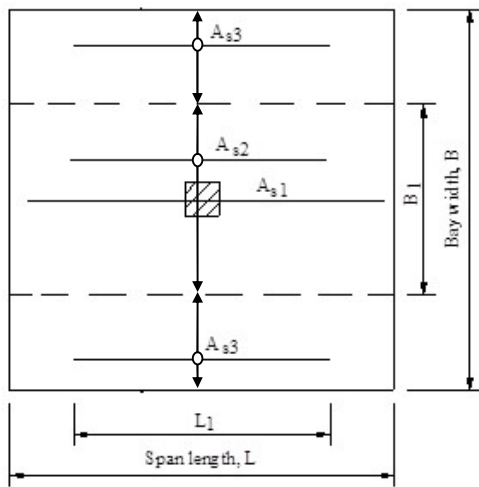


a. Specimen 8I

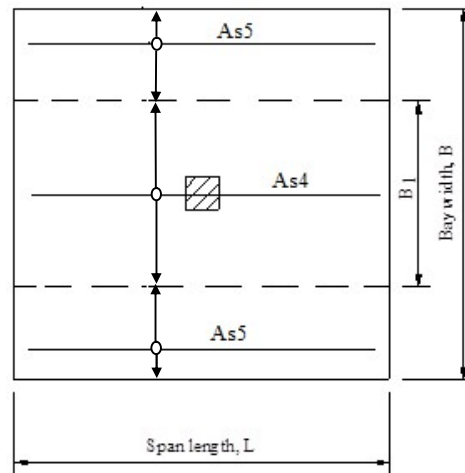


b. Specimen 9E

Fig. 3 Analytical and experimental lateral load-drift curves for specimens tested by Robertson and Durrani (1990)



Top reinforcement



Bottom reinforcement

Fig. 4 Reinforcement layout of a typical slab

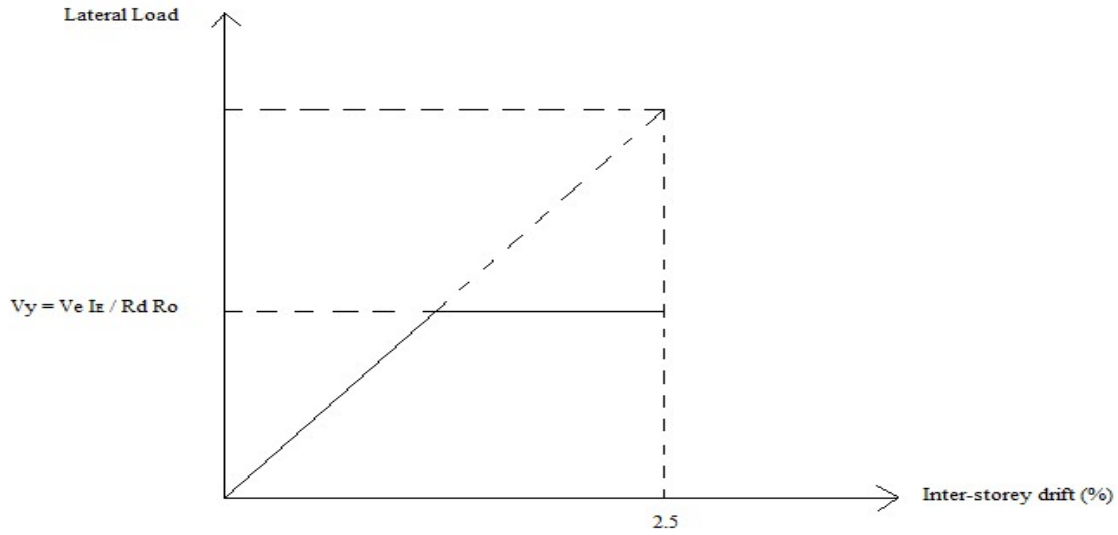


Fig. 5 Lateral load-inter-storey drift curve of a typical concrete building

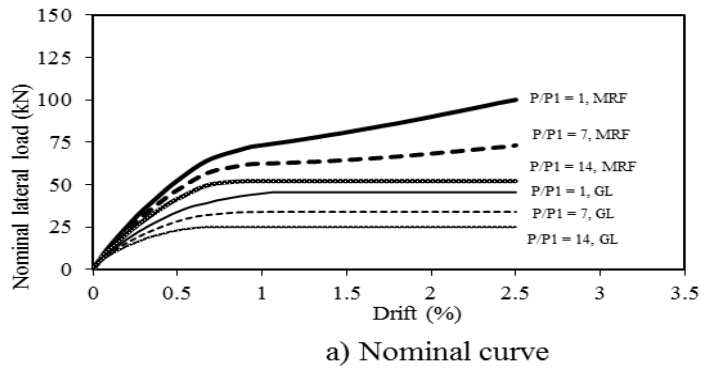


Fig. 6a Nominal lateral load-drift curves of connection C1

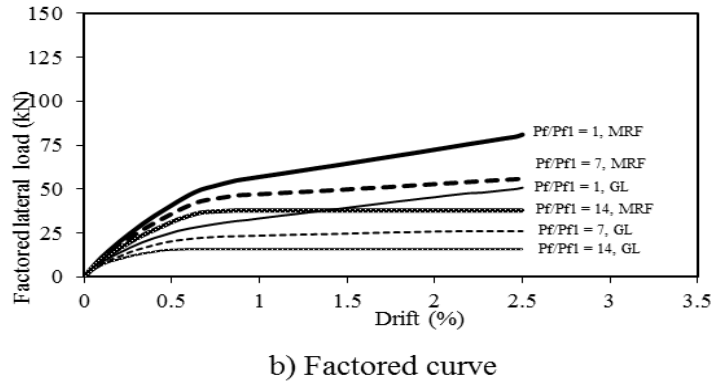
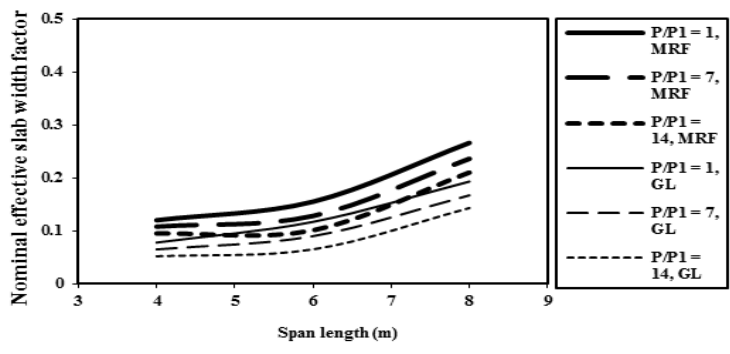
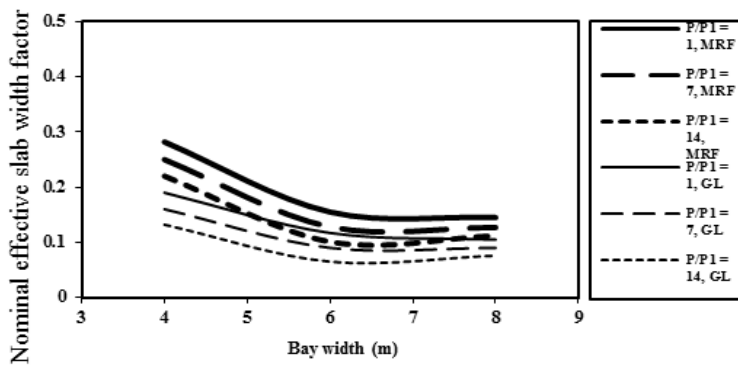


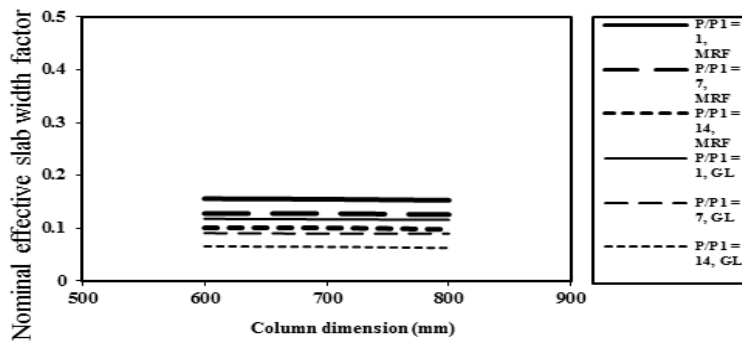
Fig. 6b Factored lateral load-drift curves of connection C1



a) Span length effect

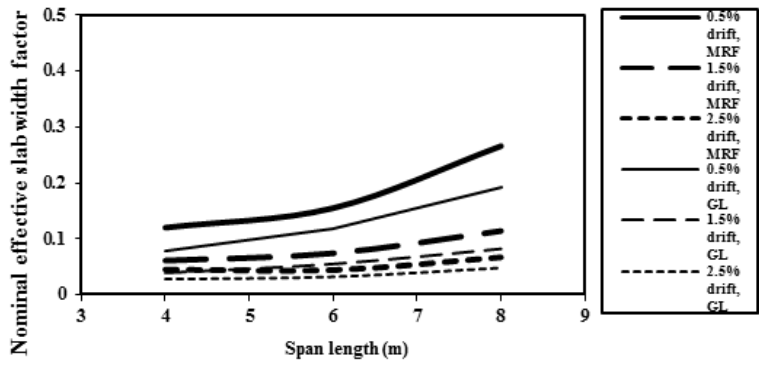


b) Bay width effect

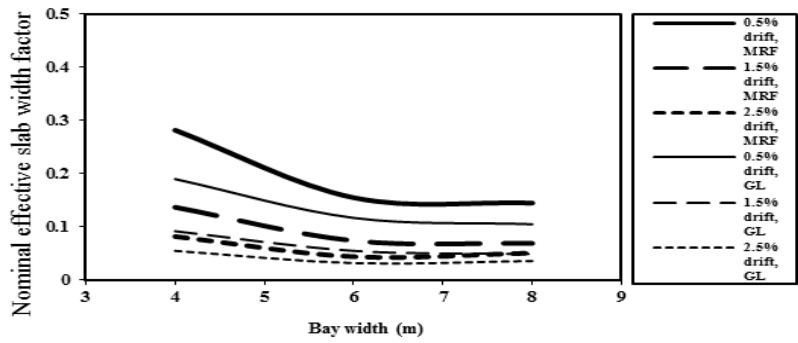


c) Column dimension effect

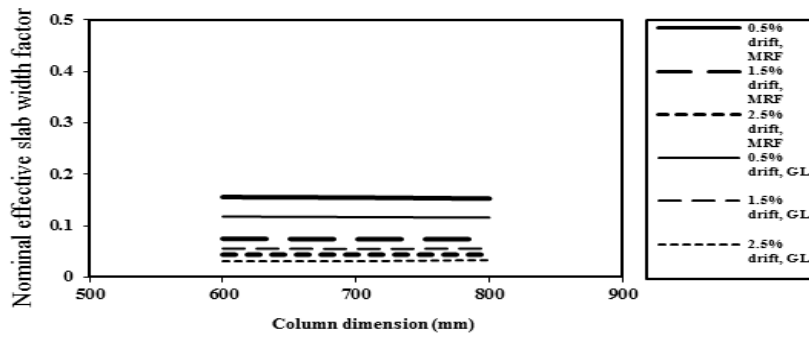
Fig. 7 Variations of effective slab width factor for nominal stiffness at 0.5 % drift



a) Span length effect

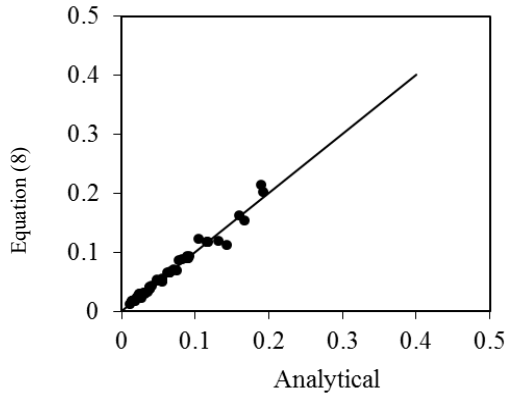


b) Bay width effect

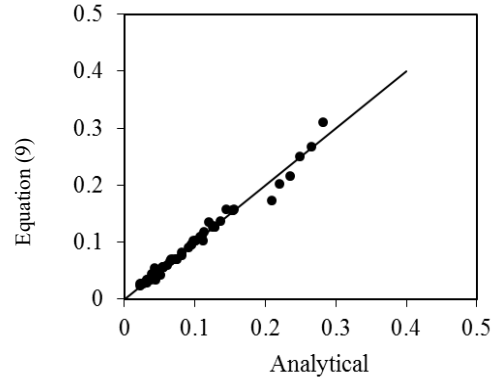


c) Column dimension effect

Fig. 8 Variations of effective slab width factor for normal stiffness at P/P1 = 1



a. Eq. 8



b. Eq. 9

Fig. 19 Predictions of equations (8 and 9) as compared to the analytical results